

# Particulate Entry Lag in Spot-Type Smoke Detectors<sup>1</sup>

THOMAS CLEARY, ARTUR CHERNOVSKY,  
WILLIAM GROSSHANDLER, and MELISSA ANDERSON  
National Institute of Standards and Technology  
Gaithersburg, Maryland, USA

## ABSTRACT

It is well documented that alarm signals from spot-type smoke detectors (ionization and photoelectric) are delayed when the threshold value has been achieved outside the detector housing as a result of convective transport of smoke through the detector to the sensing volume. This delay must be understood in order to properly design detection systems, improve fire modeling where detection is a focus, and interpret analog detector signals coming to a central panel that processes the information. Previously researchers have modeled the time-lag as a first order response with a characteristic time proportional to the inverse of velocity and a constant of proportionality defined as a characteristic length. Here, a two-parameter model is presented. The model parameters are a dwell time and a characteristic mixing time. Both parameters are correlated with velocity using a power-law equation. Detector response experiments were performed in the Fire Emulator/Detector Evaluator (FE/DE). Ceiling mounted analog output detectors were exposed to near step changes in smoke concentration over a wide range of flow velocities. Detector signals were compared to laser extinction measurements slightly forward of the detector housing. Over a flow velocity range from 0.02 m/s to 0.6 m/s, the time for detectors to achieve the maximum response ranged from seconds to 100's of seconds. The data were used to fit model parameters that exhibit strong velocity dependence at low velocities.

**KEYWORDS:** smoke detectors; fire sensing; test methods; Fire-Emulator/Detector-Evaluator

---

<sup>1</sup> This paper describes research conducted by the U.S. Department of Commerce and is not subject to copyright.

## NOMENCLATURE

$a$	proportionality constant in equation (1)
$A_e$	effective detector entrance area, $m^2$
$b$	proportionality constant in equation (2)
$c, c'$	proportionality constants in equations (1) and (2)
$E$	electrical response from smoke detector
$L_e$	effective length of plug flow region of detector, $m$
$\dot{m}$	mass flow of air into detector, $kg/s$
$Re$	Reynolds number
$t$	time, $s$
$t'$	integration constant in equation (4)
$\delta t$	dwelt time in plug flow region of detector, $s$
$u_e$	velocity of air flowing over detector, $m/s$
$V$	effective volume of sensing chamber, $m^3$
$X$	mass fraction of smoke in sensing chamber
$X_e$	mass fraction of smoke in air surrounding chamber
$Y$	extinction coefficient measured by laser light attenuation in test section, $m^{-1}$
$\nu$	kinematic viscosity of air, $m^2/s$
$\rho$	density of air, $kg/m^3$
$\tau$	characteristic time in well-mixed region of detector, $s$

## INTRODUCTION

Smoke detectors (photoelectric and ionization type) are pervasive in residential, commercial, and industrial applications. Systems with increased sensitivity are being developed and offered as early warning fire detectors, allowing for a pre-alarm level indication. In many cases, the early stage of the fire produces only a weak plume, so that the transport of smoke is slow and the air velocity adjacent to the detector may be very low. The time it takes a detector to respond to a pre-alarm level is indicative of its veracity as an early warning detector.

Advances in fluid mechanical modeling have allowed meaningful prediction of fire-induced flows such that smoke transport from a fire to a detector location in a complex geometry is possible. For performance-based codes, numerical models of the plume can lead to more efficient detector placement [1]. Conventional smoke detectors also have the potential for use as environmental particulate detectors if a way can be found to monitor and interpret the signal from the sensing unit on a continuous basis. With such capability, a "smart" fire panel could be developed to make more intelligent decisions on the fire/no fire state using the information from the full array of sensors. In the event of a fire, the smoke detectors away from the room of origin could be used in the smart panel to update a nearly real-time model prediction of the fire location and size, and the movement of smoke in the building. Displays at the smart panel could be used to direct evacuation and fire-fighting activities if the information were known to be reliable.

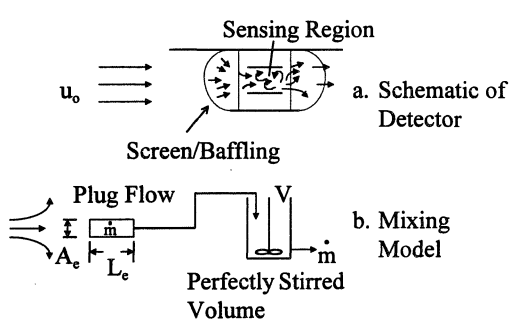
To move a smoke detector into the realm of a continuous environment sensor requires the determination of its response to known concentrations of smoke from flaming and

smoldering fires, and also to known concentrations of nuisance particulate matter (e.g., dust, water mist). This aspect of advanced detection is discussed in a recent paper by Cleary *et al.* [2]. Knowledge of the temporal response of the detector to smoke is required, as well, if the sensor output is to be related to the true environmental conditions outside of the detector body. Conventional photoelectric and ionization smoke detectors have enclosed sensing regions and do not instantaneously respond to the smoke level outside the detector. The sensing region is enclosed for various reasons including to reduce the velocity normal to the ion flow in ionization heads, to eliminate stray light in photoelectric heads, to keep out objects like bugs, and to protect the sensing element from physical damage. There are trade-offs between these considerations and a detector's temporal response; detector manufacturers are aware of these issues and have attempted to optimize their designs accordingly.

Heskestad proposed a first-order time response detector model with the characteristic time defined as  $L/u_e$  [3].  $u_e$  is the flow velocity external to the detector and  $L$  is a characteristic length, found experimentally, that depends on the physical design of the detector. Others have used the same functional form [4,5,6]. This model is adequate at sufficiently high velocities. From the low velocity experiments performed in the current study, however, it has been found that a single characteristic length is insufficient to model the time response of spot-type detectors over the full range of conditions to which they are exposed.

### DETECTOR TIME RESPONSE MODEL

An examination of a modern spot detector reveals salient geometric features that affect flow into and out of the head. Typically, the opening to the head is cylindrical and covered by a fine mesh screen. A convoluted series of baffles internally leads to a small volume where the sensing element (either an ionization or optical chamber) is located. Figure 1a shows a schematic representing the flow in a typical detector head. This arrangement suggests that the time necessary for smoke to affect the sensing element can be related to the decrease in flow caused by a pressure drop across the entrance screen and baffles, and an internal time related to the chamber volume. The incoming flow mixes into the contents of the sensing volume, and an equal amount leaves the detector (i.e., there is no build up of mass in the sensing chamber).



An idealized model of the flow is shown in Figure 1b. The amount of smoke-laden air which enters the detector,  $\dot{m}$ , depends upon the fraction of the incoming flow which is diverted by the entrance restrictions through an effective area  $A_e$ . The flow in the entrance portion of the detector is treated as moving as a slug along a distance  $L_e$ . The slug flow region empties

FIGURE 1. Schematic of flow inside the detector

into the sensing chamber, which is idealized as a perfectly-stirred region of volume  $V$ . Hence, from the series arrangement, the smoke concentration build-up depends on the dwell time during plug flow ( $\delta t$ ) and the mixing time in the sensing chamber ( $\tau$ ). The dwell and mixing times are both functions of  $\dot{m}$ , which is assumed to scale with the Reynolds number,  $Re = u_e L_e / \nu$ , to some power,  $c$ .  $\nu$  is the kinematic viscosity of air, and  $c$  is expected to be of the order of unity. Thus,

$$\delta t \equiv \frac{L_e \rho A}{\dot{m}} \approx a u_e^{-c} \quad (1)$$

and

$$\tau \equiv \frac{\rho V}{\dot{m}} \approx b u_e^{-c'} \quad (2)$$

where  $\rho$  is the density of the air,  $a$  and  $b$  are proportionality constants that account for the detector geometry and changes in ambient temperature and pressure, and  $c'$  may or may not equal  $c$ .

Let  $X$  be the mass fraction of smoke in the sensing chamber at any given time  $t$ , and  $X_e$  be the mass fraction in the air external but at the entrance to the detector. The response in the chamber at time  $t$  to a change in the environment  $\delta t$  earlier can be written

$$\rho V \frac{dX(t)}{dt} = \dot{m} \left[ X_e(t - \delta t) - X(t) \right] \quad (3)$$

If the free stream velocity is about constant and the initial mass fraction of smoke in the sensing chamber is zero, the value of  $X$  at any time later can be found by integrating equation (3) to get

$$X(t) = e^{-(t/\tau)} \int_0^{t/\tau} e^{t'/\tau} X_e \left( t' - \frac{\delta t}{\tau} \right) dt' \quad (4)$$

Particle diffusion is ignored in the above development since the molecular transport process is much too slow to impact the response (the diffusion coefficient of a 40 nm soot particle is of the order of  $3 \times 10^{-9} \text{ m}^2/\text{s}$ ). Deposition on the internal surfaces of the detector and gravitational settling are also assumed to be negligible.

Rather than the mass fraction of smoke, the extinction of laser light is more convenient to measure in the free stream. The specific extinction coefficient ( $\text{m}^2/\text{kg}$ ) is a function of the smoke aerosol size distribution and optical properties, and is an intrinsic property and nominally a constant for a given fuel and combustion mode [7]. The smoke extinction coefficient ( $\text{m}^{-1}$ ) is related to smoke mass concentration through a constant of proportionality, equal to the specific extinction coefficient.

The electrical output from the detector in response to a given mass fraction of smoke in the chamber is assumed to be directly related to the extinction of light. Combining the constants of proportionality into one,  $C$ , equation (4) can be used to relate the electrical

response from the detector,  $E(t)$ , to the light extinction (or smoke optical density) measured in the free-stream,  $Y$ :

$$E(t) = C e^{(-t/\tau)} \int_0^{t/\tau} e^{t'/\tau} Y\left(t' - \frac{\delta t}{\tau}\right) dt' \quad (5)$$

Equations (1), (2), and (5) make up the detector time response model for a varying smoke level in a constant velocity air stream. If the velocity is changing along with the smoke mass fraction but over a time scale that is long compared to  $\delta t$ , equation (3) can be integrated in an incremental fashion to account for the dependence of  $\delta t$  and  $\tau$  on the velocity.

## EXPERIMENTAL FACILITY

Experiments were performed in the NIST Fire Emulator/Detector Evaluator (FE/DE) to determine the model parameters  $a$ ,  $b$ ,  $c$  and  $c'$ . The FE/DE, first introduced by Grosshandler [8], is a flow tunnel designed to reproduce the time-varying speed, temperature and concentration (gas and particulate) expected in the plume above the early stages of a fire. This device has a test section 0.3 m high and 0.6 m wide. It has a variable speed fan and heater for velocity and temperature control over ranges of 0.02 m/s to greater than 1 m/s and 20 °C to 80 °C, respectively. It includes provisions to add water vapor, CO, CO<sub>2</sub>, and hydrocarbon gases. A honeycomb flow straightener is placed in the tunnel before the test section to calm the flow. At the test section, air temperature and velocity are measured. Laser light extinction is measured across the duct at the height of the detector inlet slightly forward of the detector placement and at the mid-height of the duct, as shown in Figure 2. Smoke concentration is uniform across the duct cross-section. A He-Ne laser at 632.8 nm wavelength is used to measure extinction. The detectors are silicon photo-diodes of the design described by Pitts, et al. [9]. The output is a signal proportional to the laser intensity reaching the detector. With the use of a stable laser and additional laser intensity stabilization, the signal to noise ratio is approximately 10<sup>4</sup>:1 with no smoke present. The signal is normalized by the pre-test signal level and recorded as a relative intensity ratio at 1 s intervals. The laser is reflected off two mirrors inside the tunnel to extend the path length to 1.50 m. Smoke deposition on these mirrors produces a slight positive baseline drift. The magnitude of this offset depends on the smoke concentration and test time.

A propene diffusion burner provides a black smoke (soot) source. The smoke generator was operated between a range of fuel flow and co-flowing air of 0.3 cm<sup>3</sup>/s to 25 cm<sup>3</sup>/s, and 500 cm<sup>3</sup>/s to 1700 cm<sup>3</sup>/s, respectively. The burner flow settings for each test were fixed. A portion of the flow from the smoke generator was injected into the flow tunnel upstream from the test section to achieve the desired smoke concentration. Step changes in smoke concentration up to 20 %/m obscuration can be achieved. The smoke output from the burner is stable for at least 30 minutes. Temperature increase at the test section is less than 3 °C for these tests. The tunnel has a top-hat mean velocity profile at low flows (up to 0.3 m/s) and then starts to develop a parabolic profile at higher flows. At the location of the detector opening (two to three cm below the ceiling of the tunnel) the vertical velocity gradient is small. Velocity was measured with a hot-wire anemometer calibrated from 0.05

m/s to 5 m/s. Measurements of flow velocities less than 0.05 m/s were obtained from neutrally buoyant soap bubble trajectories and punk smoke visualization. Measurement uncertainty is estimated at  $\pm 10\%$  of the value for velocities greater than 0.05 m/s using the hot-wire anemometer, and  $\pm 25\%$  for speeds below 0.05 m/s.

The detectors examined in this study, supplied by two different commercial sources, had photoelectric or ionization sensors. They are identified as P1, P2, I1, and I2 for photoelectric (P) and ionization (I) models and manufacturers (1 and 2). All detector housings were physically different. For these detectors, the output signal is available at approximately 5 s intervals. This interval is fixed by the head communications polling and

processing time delay in the manufacturer-supplied control panel. Detector output signals are transmitted as 8-bit binary numbers allowing for a resolution of 1 in 256. The detectors were mounted at the center of the flow tunnel ceiling in the test section (Figure 2). Both ionization and photoelectric detector output were found to be linear functions of optical density for the smoke produced by the propene diffusion burner, suggesting that the detector electronics were linearized internally by the manufacturers with respect to optical density.

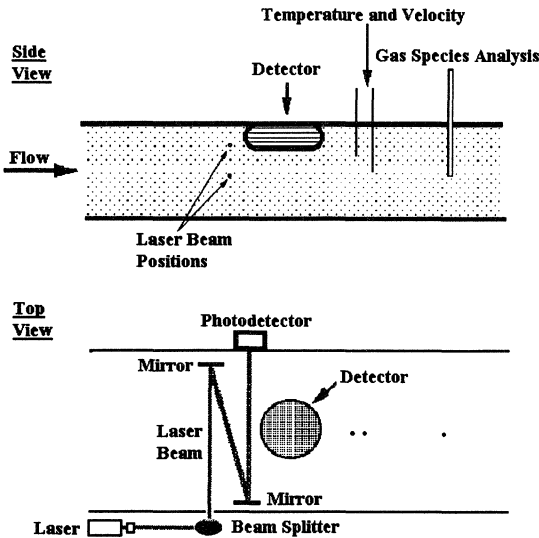


FIGURE 2. Schematic of FE/DE test section

## RESULTS AND ANALYSIS

The response of all the detectors was examined when a step change in smoke concentration was instituted in the FE/DE. Figure 3 is a typical example, with time in seconds plotted on the abscissa, the smoke extinction coefficient measured by laser light attenuation in the FE/DE on the right-hand ordinate, and the detector electrical output on the left-hand ordinate. The damper was opened at 60 s to introduce the smoke. This does not cause a measurable change in the nominal airflow at the detector, which is set at  $0.20 \text{ m/s} \pm 0.02 \text{ m/s}$  for this particular test. The leading edge of the smoke concentration wave arrives at 74 s, rises in less than 10 s to a maximum of  $0.023 \text{ m}^{-1} \pm 0.003 \text{ m}^{-1}$ , and remains about constant for over 150 s. The smoke damper is closed after the steady concentration period; soon after (at 250 s) the trailing edge of the smoke wave can be detected at the test section. The smoke concentration in the test section approaches its original pristine level within the next 10 s.

The dotted line in Figure 3 is drawn through the discrete output of the photoelectric detector, P1, represented by the open squares. The detector signal is in arbitrary units, with a baseline of  $62 \pm 1$ . The sensor responds to the arrival of the smoke in less than 10s. The output increases almost in parallel with the smoke levels measured outside of the detector, reaches a maximum of  $85 \pm 3$ , and follows the step decrease in external smoke concentration in a mirror image of the increase. For an air velocity as high as 0.2 m/s, a simple displacement in time of about 8 s appears to be sufficient to relate the detector response to the external environmental state.

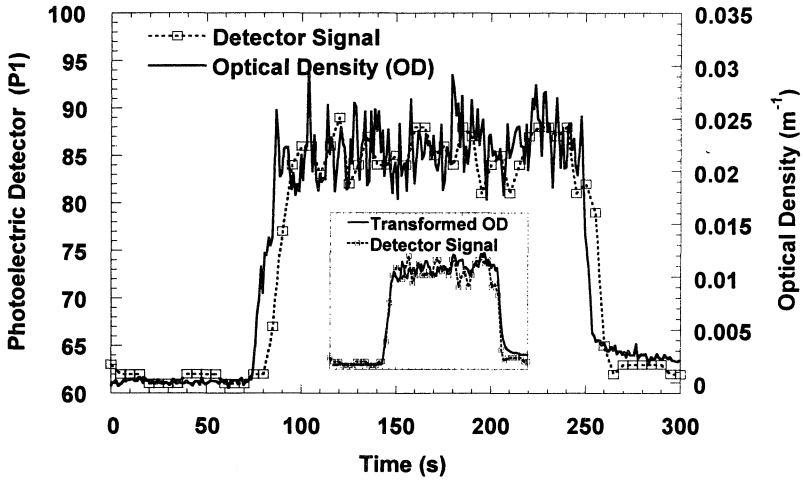


FIGURE 3. Response of detector P1–flow velocity is 0.20m/s, smoke damper opened 60s

The same photoelectric detector was tested at a nominal air speed of 0.02 m/s. Figure 4 is a plot of the result, showing a number of differences from the higher speed test. The environment in the test section of the FE/DE exhibits a slower rise in the measured extinction coefficient (solid line) and a higher level of smoke, indicative of a larger fraction of flow originating from the smoke generator. The first response of the detector occurs well over 100 s after the smoke begins building up in the environment. The peak output of the detector (about 136) reflects the higher smoke level, but it never attains the plateau in concentration measured external to the detector. The decrease in signal from P1 resulting from the drop in external smoke levels does not appear as a mirror image of the increase. In fact, at one point the drop in output exceeds the rate at which the environmental smoke is decreasing. Since the signal from the sensor passes through a proprietary algorithm before the output is displayed, it is not possible to directly relate the data plotted as open squares in Figure 4 to the actual concentration of smoke in the sensing volume.

The response of photoelectric detector P2, from a different manufacturer, is shown in Figure 5. The nominal airflow is 0.03 m/s. The plug flow and well-stirred character of this detector are easily distinguished by comparing the shapes of the solid and dotted lines, which represent the smoke levels external to the detector and within the sensing chamber,

respectively. The shift in time scale is related to the plug flow dwell time, and the decrease in rate-of-rise is associated with the residence time associated with the well-stirred region.

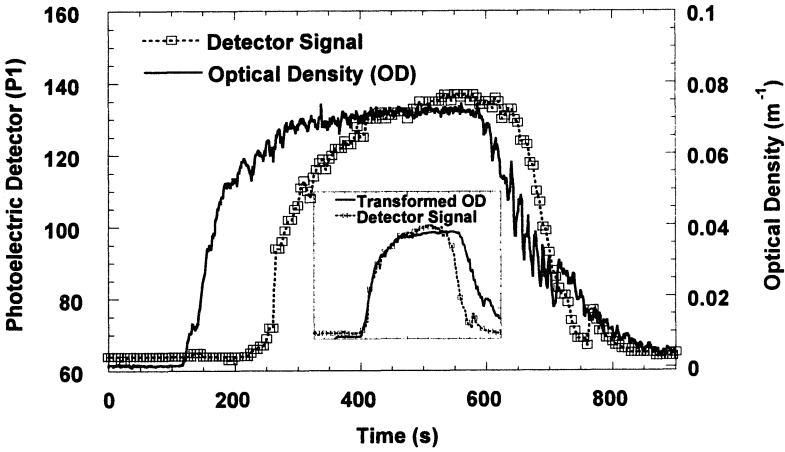


FIGURE 4. Response of detector P1 – flow velocity is 0.02m/s, smoke damper opened 60s

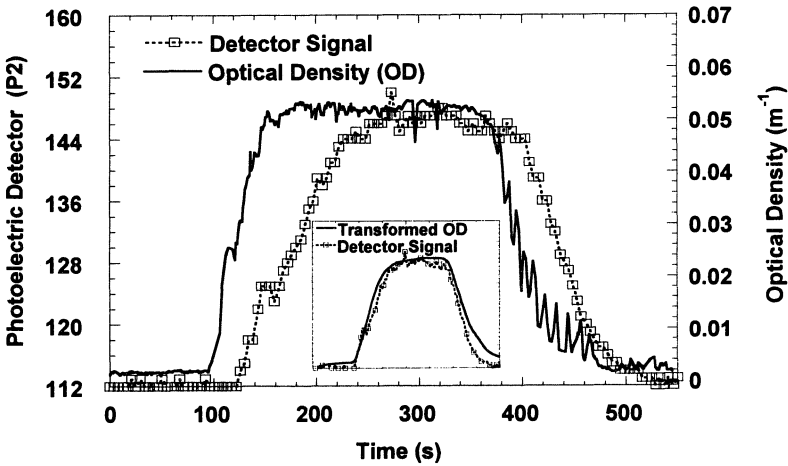


FIGURE 5. Response of detector P2 – flow velocity is 0.03m/s, smoke damper opened 60s

Figures 6 and 7 compare the response of two different ionization detectors, I1 and I2. The smoke is able to enter the ion chamber of I1 much more quickly than it enters I2. While some of the difference is attributable to the higher airflow in Figure 6 (0.05 m/s versus 0.03 m/s in Figure 7), there is an approximately factor of four difference in delay times between the two designs.



The data from about 25 tests over a range of velocities between 0.02 m/s and 0.55 m/s were used to establish the values of  $a$ ,  $b$ ,  $c$  and  $c'$  in equations (1) and (2) for each of the four detectors evaluated in the current study. The process for fitting the curves is done manually in two steps. First, the measured extinction coefficient curve is time-shifted to the right to match up with the respective detector output such that the initial rise in each curve matches; this time shift is recorded as the dwell time,  $\delta t$ . A rough estimate of the time constant,  $\tau$ , is made and the integration and multiplication of the right hand side of equation (5) is performed on the data file. This transformation is repeated with  $\tau$  updated to provide improved matching of the curves. The y-axis scale factor is determined from the ratio of the differences in the peak values and the baselines for the two curves. This operation will be automated in the future to streamline the process of determining  $\tau$  and  $\delta t$  over the range of velocities.

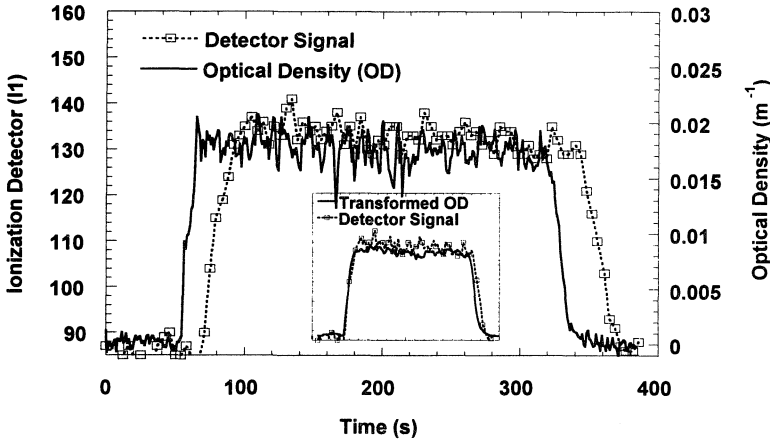


FIGURE 6. Response of detector I1 - flow velocity is 0.05m/s, smoke damper opened 30s

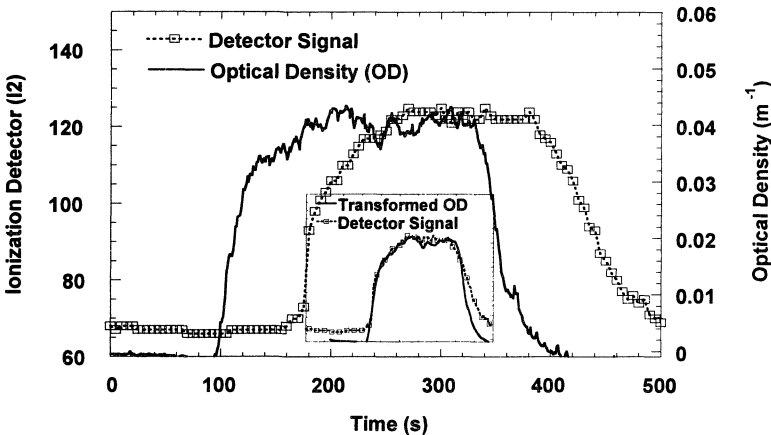


FIGURE 7. Response of detector I2 - flow velocity is 0.03 m/s, smoke damper opened 60s

The small inserts in Figures 3 through 7 show how well the transformed signals from the laser attenuation measurements in the FE/DE test section track the electrical responses of the four detectors examined. Except for Figure 4, where the decrease in detector signal on the back side of the smoke wave precedes the drop in the environmental state, the two parameter model is able to account for the physical processes that control the transport of smoke from the environment to the sensing chamber.

The dwell time (open squares) and mixing time (triangles) for P1 are plotted in Figure 8 as a function of the air velocity. The strong dependence of each on the airflow as the velocity decreases below 0.1 m/s is evident. At an air velocity greater than 0.5 m/s, the dwell time drops below 10 s and the mixing time is essentially zero, indicating that a single parameter model is sufficient for high airflow, at least for this particular detector design. If equations (1) and (2) are used to fit the data, the dotted and solid lines in Figure 8 are the result; R is the correlation coefficient for the best fit curve. There is significant scatter in the model parameters, some of it due to the uncertainty in measured flow velocity. Also, the internal baffling in P1 is not radially symmetrical, making the results subject to the relative direction of the approach velocity. As anticipated, the exponent on the velocity for both  $\tau$  and  $\delta t$  is close to -1. By dividing  $\delta t$  by  $\tau$ , the relative size of the plug flow region ( $L_e A_e$ ) to the well-mixed region ( $V$ ) can be estimated to be  $(1.8 u_e^{-1.0}) / (0.97 u_e^{-0.76})$ , or approximately  $1.8 u_e^{-0.24}$ . Over the range of velocities examined, the ratio is of the order of two.

Figures 9 through 11 are plots of  $\delta t$  and  $\tau$  for the other detectors, P2, I1, and I2. The general behavior of P2 is the same as for the other photo-detector, although both time constants are slower for P1. The ratio of the plug flow to the well-mixed region is close to 2.5:1 for P2. The values of the parameters found for I2 are essentially identical to those found for P1, while the best fit of the data for I1, suggests a lesser fall off with velocity for  $\delta t$ .

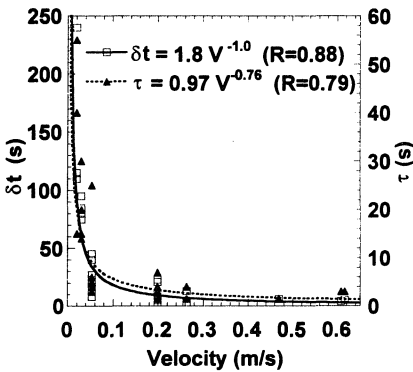


FIGURE 8. Model parameters for P1

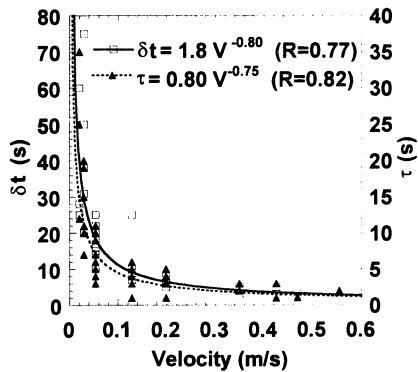


FIGURE 9. Model parameters for P2

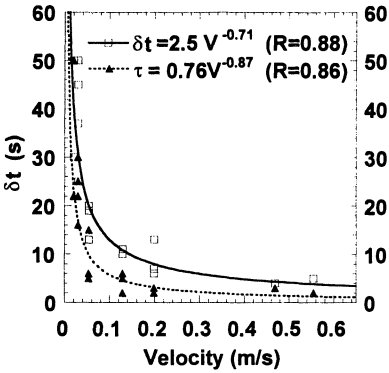


FIGURE 10. Model parameters for I1

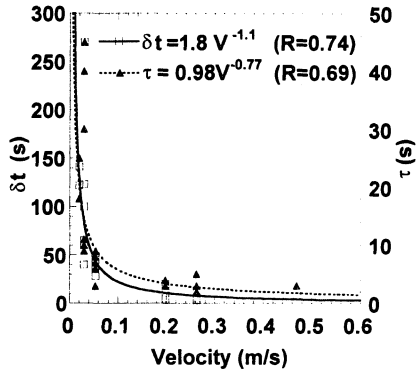


FIGURE 11. Model parameters for I2

## SUMMARY AND CONCLUSIONS

The design of conventional spot-type smoke detectors requires that particulate matter from the external environment be transported to the internal sensing chamber by natural means. The associated delay in response is known to be a strong function of the velocity of the air moving over the detector head. To make maximum use of the information provided by the detector, it is necessary to relate the electrical signal at any given time to the actual conditions in the air adjacent to the detector. This can be done if one knows how a particular detector responds to a time varying concentration of smoke in the air stream.

The Fire-Emulator/Detector-Evaluator has been used in the current study to produce an environment for ionization and photo-electric spot detectors in which the smoke levels, temperature and velocity were controlled over a range of conditions typical of the early stage of a flaming fire. By imposing a step change in smoke levels, as measured by laser light extinction, the time response of the detectors was measured. Response times varied from less than 5 s at the highest flows examined to well over 100 s for the slowest air velocities.

A two-parameter model, based on a physical description of a generic detector head, has been proposed assuming plug flow and perfectly stirred behavior occur in series within the detector head. The velocity dependence is described adequately over a flow range from 0.02 to 0.6 m/s with the correlation. The model is recommended for situations in which the velocity is changing, as well, and should be able to deal with moderate changes in density and temperature through the proportionality constants in equations (1) and (2).

## REFERENCES

1. Davis, W., Forney, G., Bukowski, R., "Developing Detector Siting Rules from Computational Experiments in Spaces with Complex Geometries," Fire Safety Journal, Vol. 29, pp. 129-139, 1997.
2. Cleary, T., Grosshandler, W., and Chernovsky, A., "Smoke Detector Response to Nuisance Aerosols," International Conference on Automatic Fire Detection "AUBE '99", 11th, March 16-18, 1999, Gerhard Mercator University, Duisburg, Germany, Luck, H., Editor, pp. 32-41, 1999.
3. Heskestad, G., "Generalized Characterization of Smoke Entry and Response for Products of Combustion Detectors," Proceedings of the Fire Detection for Life Safety Symposium, March 31- April 1, 1975.
4. Newman, J.S., "Prediction of Fire Detector Response," Fire Safety Journal, Vol. 12, pp. 205-211, 1987.
5. Bjorkman, J., Kokkala, M.A., and Ahola, H., "Measurements of the Characteristic Lengths of Smoke Detectors," Fire Technology, pp. 99-109, May 1992.
6. Oldweiler, A. J., "Investigation of the Smoke Detector L-Number in the UL Smoke Box," M.S. Thesis, Worcester Polytechnic Institute, Worcester MA, May 1995.
7. Mulholland, G., "How Well Are We Measuring Smoke?" Fire and Materials, Vol. 6, No. 2, pp. 65-67, 1982.
8. Grosshandler, W., "Towards the Development of a Universal Fire Emulator-Detector Evaluator," Fire Safety Journal, Vol. 29, pp. 113-128, 1997.
9. Pitts, W., Yang, J., Gmurczyk, G., Cooper, L., Grosshandler, W., Cleveland, W., and Presser, C., "Fluid Dynamics of Agent Discharge," Section 3 in Evaluation of Alternative In-Fight Fire Suppressants for Full-Scale Testing in Simulated Aircraft Engine Nacelles and Dry Bays, Grosshandler, W., Gann, R., and Pitts, W., editors, NIST Special Publication SP 861, National Institute of Standards and Technology, U.S. Dept. of Commerce, Gaithersburg, MD, 1994.